04

Concentration and mobility of charge carriers in the superionic conductor $Ba_{1-x}La_xF_{2+x}$ $(0.05 \leq x \leq 0.5)$

© N.I. Sorokin

Shubnikov Institute of Crystallography „Crystallography and Photonics“, Russian Academy of Sciences, Moscow, Russia

E-mail: nsorokin1@yandex.ru

Received November 14, 2023
Revised November 14, 2023
Accepted November 29, 2023

The frequency-temperature dependences of alternating current conductivity $\sigma_{ac}(\nu, T)$ for concentration series of single crystals of nonstoichiometric superionic conductor $Ba_{1-x}La_xF_{2+x}$ $(0.05 \leq x \leq 0.5)$ with the fluorite structure (sp. gr. $Fm\bar{3}m$) were investigated. The electrophysical measurements carried out in the frequency range $10^{-1}-10^{7}$ Hz and temperature range 210–409 K. From the analysis of the curves $\sigma_{ac}(\nu, T)$ we obtained the concentration dependences of conductivity $\sigma_{dc}(x)$, average frequency of charge carrier jumps $\nu_h(x)$, enthalpies of activation of conductivity $\Delta H_\sigma(x)$ and hopping frequency $\Delta H_h(x)$. The mobility $\mu_{mob}(x)$ and concentration $n_{mob}(x)$ of charge carriers (mobile interstitial ions F'_{mob}) are calculated within the framework of crystallophysical model. The dependences $\sigma_{dc}(x)$, $n_{mob}(x)$ and $\mu_{mob}(x)$ are symbatic. It was found that contributions of the mobility $\mu_{mob}(x)$ and concentration $n_{mob}(x)$ of charge carriers to the concentration dependence of the „room“ conductivity $\sigma_{dc}(x)$ of the $Ba_{1-x}La_xF_{2+x}$ superionic conductor were almost identical, when the composition changes from $x = 0.05$ to $x = 0.5$.

Keywords: superionic conductivity, single crystals, barium and lanthanum fluorides, solid solutions, fluorite structure, point defects.

DOI: 10.61011/PSS.2024.01.57854.253

1. Introduction

This study continues our publications [1–4] related to the investigation of microscopic parameters of charge carriers responsible for superionic conductivity in nonstoichiometric fluorides. Nonstoichiometric phase (heterovalent solid solution) $Ba_{1-x}La_xF_{2+x}$ is a model system for fluoride superionic conductors. High-conducting and thermostable $Ba_{1-x}La_xF_{2+x}$ crystals became the most important materials for the study of the heterovalent isomorphism effect on the ionic transport in inorganic fluorides [5–13]. Studies of ionic transport in $Ba_{1-x}La_xF_{2+x}$ superionic conductor crystals are summarized in [1].

Introduction of LaF_3 impurity component into BaF_2 fluorite matrix (type CaF_2, space group $Fm\bar{3}m$) results in formation of nonstoichiometric phase $Ba_{1-x}La_xF_{2+x}$ $(0 < x \leq 0.52)$ with limit concentration of 52 ± 2 mol.% LaF_3 in the condensed BaF_2-LaF_3 system [14] at an eutectic temperature of 1663 ± 5 K. Heterovalent substitutions of Ba^{2+} cations by La^{3+} induce high concentration of „crystallochemical“ point defects in the fluorite structure of this solid solution. With crystal cooling, the concentration of „crystallochemical“ defects is maintained.

A single-crystal form is most suitable for investigation of fundamental properties of superionic conductors. $Ba_{1-x}La_xF_{2+x}$ solid solution single-crystals are grown from melt by the directional solidification techniques [15]. At low concentration of LaF_3 $(x < 0.01)$, nnn-[next near neighbor] dipoles primarily occur in the crystals and consist of $La^{\bullet}_{Ba}$ defect and interstitial ion F'_i located in the second coordination sphere of the cation [16–18]. Here, the defects are denoted in the Kröger–Wink system [19].

With growing concentration of LaF_3 in the solid solution, point defects are condensed into structural clusters containing several rare-earth cations. $[R_6F_{37}]$ type octahedral clusters [20] or $[Ba_8(R_6F_{37})F_{32}] = [Ba_8R_6F_{69}]$ octahedral-cubic clusters [21,22] formed on their basis are offered as the most probable model of structural clusters in $Ba_{1-x}R_xF_{2+x}$ solid solutions (R — rare earth elements). The existence of $[Ba_8R_6F_{69}]$ clusters is confirmed by the investigation of nonstoichiometric phases $Ba_{1-x}R_xF_{2+x}$ by the electron paramagnetic resonance [23,24] and elastic neutron scattering [25] methods as well as by the X-ray diffraction analysis of ordered phases $Ba_4R_3F_{17}$ $(R = Yb, Y)$ [26] where the lattice cell contains three such clusters.

$Ba_{1-x}La_xF_{2+x}$ solid solution is a perfect example of the effect exercised on the ion-conducting properties of fluoride crystals by the heterovalent isomorphism that transforms the anion sublattice into a superionic state. Concentration dependence of the direct current conductivity $\sigma_{dc}(x)$ for $Ba_{1-x}La_xF_{2+x}$ solid solution (on single-crystals) was studied in [9,10,13]. These studies found the growth of conductivity of fluorite solid solution with increasing concentration of LaF_3. Electronic conductivity of BaF_2 and solid solutions on its basis is low, therefore, compared with ionic conductivity, it may be neglected [9,27]. Therefore, $Ba_{1-x}La_xF_{2+x}$ solid solution may be treated as promising fluorine-conducting solid electrolyte, gas sensor for HF

recording [28] and fluorine-ionic current sources on its basis were offered [8,29,30].

We have earlier studied in detail the temperature dependences of ionic conductivity $\sigma_{dc}(T)$ of $Ba_{1-x}La_xF_{2+x}$ $(0.05 \le x \le 0.5)$ crystals in the range of 324–1073 K [9]. Therefore, $Ba_{1-x}La_xF_{2+x}$ crystals were chosen as a model system for measurement of the frequency dependences of the alternating current conductivity $\sigma_{ac}(\nu)$ and for calculation of microscopic parameters of superionic conductivity (hopping frequency ν_h and distance d_h, charge carrier mobility μ_{mob} and concentration n_{mob}). In [1], we used this approach to study fluorine ion mobility in $Ba_{0.69}La_{0.31}F_{2.31}$ crystal whose composition corresponds to the peak $(1757 \pm 10\,K$ [10]) on melting curves and has congruent melting.

The objective of this study was to investigate frequency-temperature dependences of the alternating current conductivity $\sigma_{ac}(\nu, T)$ of $Ba_{1-x}La_xF_{2+x}$ superionic conductor single-crystals in a wide composition variation range $(0.05 \le x \le 0.5)$ and to find concentration dependences $\mu_{mob}(x)$ and $n_{mob}(x)$ of charge carriers.

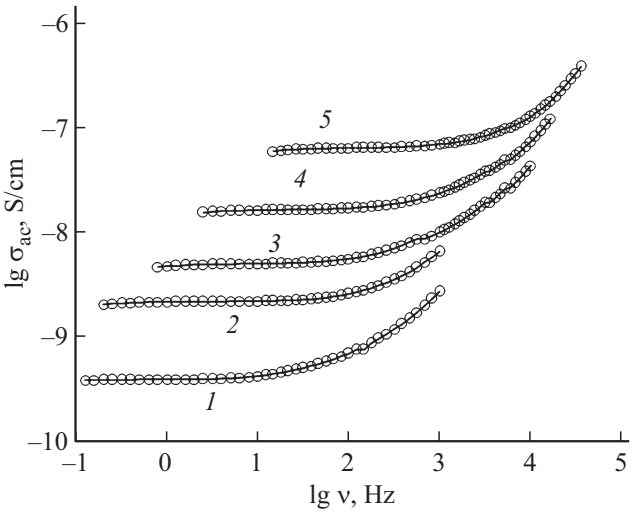

Figure 1. Frequency dependences of conductivity $\lg\sigma_{ac}(\nu)$, $\lg\nu$ for $Ba_{1-x}La_xF_{2+x}$ crystals at x equal to 0.05 (curve *1*), 0.15 (*2*), 0.25 (*3*), 0.325 (*4*), 0.50 (*5*). The temperature is equal to 292 ± 1 K.

2. Frequency-temperature dependences of conductivity of $Ba_{1-x}La_xF_{2+x}$ $(0.05 \le x \le 0.5)$ superionic conductor

Crystal growing procedure for $Ba_{1-x}La_xF_{2+x}$ solid solution is described in detail in [15]. Single-crystals with $x = 0.05$, 0.15, 0.25, 0.325 and 0.5 were produced from melt by the vertical Bridgman directional solidification in fluorinating atmosphere provided by polytetrafluorethylene pyrolysis products. The fluorinating atmosphere is necessary to suppress pyrohydrolysis reaction that is typical for fluorides. Cubic macrosymmetry and $Ba_{1-x}La_xF_{2+x}$ crystal affiliation with the fluorite structural type (CaF_2 type, space group $Fm\bar{3}m$) was confirmed by the radiographic technique. X-ray diffraction investigations were carried out using HZG-4 (CuK_α emission, Si internal standard) diffractometer. No impurity phases were detected on the X-ray images.

Chemical composition (x) of crystals was determined by the concentration dependence of the lattice cell parameter $a = f(x)$ for fluorite phase $Ba_{1-x}La_xF_{2+x}$ [14] and corresponded to the initial charge composition with accuracy $\Delta x = \pm 0.01$ (± 1 mol.% LaF_3). Oxygen impurity content in the crystals was 0.01–0.02 mass.%.

Samples for electrophysical studies were prepared in the form of a cube 5 mm on side, with all faces polished. They were of high quality (Zeiss KL1500 optical microscope) and contained no microinclusions. Sample orientation in crystallographic axis was not conducted, because $Ba_{1-x}La_xF_{2+x}$ crystals have cubic crystal system and isotropic conductivity behavior. Leitsilber silver paste was applied to the effective surfaces of samples as electrodes.

Conductivity $\sigma_{ac}(\nu)$ was measured by the alternating current method (Solartron 1260 impedancemeter, frequency range 10^{-1}–10^5 Hz, voltage 30 mV). Electrophysical measurements were conducted with cooling in the temperature range from 409 to 210 K in vacuum $\sim 10^{-3}$ Pa. Conductometric measurement error was max. 2%. The experimental setup is described in [2].

Figure 1 shows frequency dependences $\sigma_{ac}(\nu)$ for $Ba_{1-x}La_xF_{2+x}$ single-crystals with $x = 0.05$–0.5 at room temperature. In the low frequency range, curves $\sigma_{ac}(\nu)$ have a frequency-independent conductivity that corresponds to the direct current conductivity σ_{dc}. With increasing frequency, conductivity increases exponentially $\sigma_{ac}(\nu) \propto \nu^n$, where $0 < n < 1$. With temperature growth, section $\sigma_{ac}(\nu)$ corresponding to σ_{dc} moves towards high frequencies, however, the low frequency range shows polarization processes of charge accumulation on phase boundaries of electrochemical system $Ag - Ba_{1-x}La_xF_{2+x}$ (not shown in Figure 1).

Frequency dependences of conductivity for superionic $Ba_{1-x}La_xF_{2+x}$ are explained by the charge carrier hopping migration mechanism [31]:

$$\sigma_{ac}(\nu) = \sigma_{dc}[1 + (\nu/\nu_h)^n], \quad (1)$$

where ν_h is the mean charge carrier hopping frequency that characterizes charge carrier distribution by frequencies (energies). Ion carriers participate in electrical conductivity when $\nu < \nu_h$ and in dielectric relaxation when $\nu > \nu_h$. When $\nu = \nu_h$, the following equation is satisfied

$$\sigma_{ac}(\nu_h) = 2\sigma_{dc}. \quad (2)$$

Values of σ_{dc} and ν_h at room temperature calculated by mathematical processing of $\sigma_{ac}(\nu)$ by equations (1) and (2) are listed in Table 1.

Figure 2 shows temperature dependences of ionic conductivity $\sigma_{dc}(T)$ for given $Ba_{1-x}La_xF_{2+x}$ single-crystals.

Table 1. Direct current conductivity σ_{dc}, mean hopping frequency ν_h, charge carrier mobility μ_{mob} and hopping distance d_h in $Ba_{1-x}La_xF_{2+x}$ superionic conductor at room temperature (experiment)

Crystal	T, K	σ_{dc}, S/cm	ν_h, Hz	μ_{mob}, $cm^2/(sV)$	d_h, nm
$Ba_{0.95}La_{0.05}F_{2.05}$	290.7	$4.0 \cdot 10^{-10}$	$6.8 \cdot 10^{1}$	$1.8 \cdot 10^{-11}$	2.0
$Ba_{0.85}La_{0.15}F_{2.15}$	292.7	$2.2 \cdot 10^{-9}$	$2.6 \cdot 10^{2}$	$3.2 \cdot 10^{-11}$	1.3
$Ba_{0.75}La_{0.25}F_{2.25}$	292.1	$5.0 \cdot 10^{-9}$	$4.7 \cdot 10^{2}$	$4.3 \cdot 10^{-11}$	1.2
$Ba_{0.675}La_{0.325}F_{2.325}$	292.0	$1.6 \cdot 10^{-8}$	$1.1 \cdot 10^{3}$	$1.0 \cdot 10^{-10}$	1.2
$Ba_{0.5}La_{0.5}F_{2.5}$	292.6	$6.2 \cdot 10^{-8}$	$5.6 \cdot 10^{3}$	$2.5 \cdot 10^{-10}$	0.8

Table 2. Parameters in equations (3) and (4) for the ionic conductivity and charge carrier hopping frequency in $Ba_{1-x}La_xF_{2+x}$ superionic conductor

Crystal	σ_0, 10^5 SK/cm	H_σ, eV, ± 0.01	ν_0, 10^{13} Hz	H_h, eV, ± 0.03
$Ba_{0.95}La_{0.05}F_{2.05}$	11.6	0.75	2.3	0.67
$Ba_{0.85}La_{0.15}F_{2.15}$	1.6	0.66	1.8	0.63
$Ba_{0.75}La_{0.25}F_{2.25}$	2.0	0.64	3.2	0.63
$Ba_{0.675}La_{0.325}F_{2.325}$	1.9	0.61	1.9	0.59
$Ba_{0.5}La_{0.5}F_{2.5}$	2.8	0.59	2.6	0.56

Table 3. Direct current conductivity σ_{dc}, concentration n_{mob} and mobility μ_{mob} of charge carriers in $Ba_{1-x}La_xF_{2+x}$ superionic conductor (calculation)

Crystal	σ_{dc}, S/cm		μ_{mob}, $cm^2/(sV)$		n_{mob}, cm^{-3}
	293 K	400 K	293 K	400 K	
$Ba_{0.95}La_{0.05}F_{2.05}$	$5.0 \cdot 10^{-10}$	$1.0 \cdot 10^{-6}$	$2.2 \cdot 10^{-11}$	$4.5 \cdot 10^{-8}$	$1.4 \cdot 10^{20}$
$Ba_{0.85}La_{0.15}F_{2.15}$	$2.4 \cdot 10^{-9}$	$2.0 \cdot 10^{-6}$	$3.5 \cdot 10^{-11}$	$2.9 \cdot 10^{-8}$	$4.3 \cdot 10^{20}$
$Ba_{0.75}La_{0.25}F_{2.25}$	$5.8 \cdot 10^{-9}$	$3.9 \cdot 10^{-6}$	$5.0 \cdot 10^{-11}$	$3.3 \cdot 10^{-8}$	$7.3 \cdot 10^{20}$
$Ba_{0.675}La_{0.325}F_{2.325}$	$1.8 \cdot 10^{-8}$	$8.8 \cdot 10^{-6}$	$1.2 \cdot 10^{-10}$	$5.8 \cdot 10^{-8}$	$9.5 \cdot 10^{20}$
$Ba_{0.5}La_{0.5}F_{2.5}$	$6.8 \cdot 10^{-8}$	$2.6 \cdot 10^{-5}$	$2.8 \cdot 10^{-10}$	$1.1 \cdot 10^{-7}$	$1.5 \cdot 10^{21}$

Curves $\sigma_{dc}(T)$ satisfy the Frenkel–Arrhenius equation:

$$\sigma_{dc} = (\sigma_0/T)\exp[-H_\sigma/kT], \quad (3)$$

where σ_0 is the pre-exponential conductivity factor, H_σ is the ion transport activation enthalpy. Enthalpy H_σ and ionic conductivity σ_{dc} are listed in Tables 2 and 3. At 400 K, ionic conductivity of $Ba_{0.5}La_{0.5}F_{2.5}$ crystal is equal to $\sigma_{dc} = 2.6 \cdot 10^{-5}$ S/cm and is $\sim 10^9$ times greater than the intrinsic conductivity of BaF_2 crystal ($4 \cdot 10^{-15}$ S/cm [32]).

Mean charge carrier hopping frequency ν_h is of activation type and its temperature dependences for $Ba_{1-x}La_xF_{2+x}$ crystals correspond to the Arrhenius type equation (Figure 3):

$$\nu_h = \nu_0 \exp[-H_h/kT], \quad (4)$$

where ν_0 is the pre-exponential factor of hopping frequency and H_h is the anion carrier hopping activation enthalpy. Charge hopping frequency $\nu_h(x)$ and enthalpy H_h are listed in Tables 1 and 2.

3. Concentration dependences of microscopic parameters of charge carriers in $Ba_{1-x}La_xF_{2+x}$ superionic conductor ($0.05 \le x \le 0.5$)

In $Ba_{1-x}La_xF_{2+x}$ superionic conductor with a fluorite structure, hopping conductivity mechanism is implemented and anion carriers participate in charge transport in thermal activation conditions [33]. Ionic conductivity of $Ba_{1-x}La_xF_{2+x}$ crystals is determined by the product of concentration and mobility of charge carriers

$$\sigma_{dc} = qn_{mob}\mu_{mob} = (qn_0\mu_0/T)\exp\left[-(H_f + H_h)/kT\right], \quad (5)$$

where q is the charge, n_0 and μ_0 are pre-exponential factors of concentration and mobility, respectively, H_f is the anion carrier formation enthalpy, other designations were explained earlier.

Coincidence of conductivity activation and carrier hopping frequency enthalpies is observed within the experimental accuracy: $H_\sigma \approx H_h$ (Table 2). This fact shows

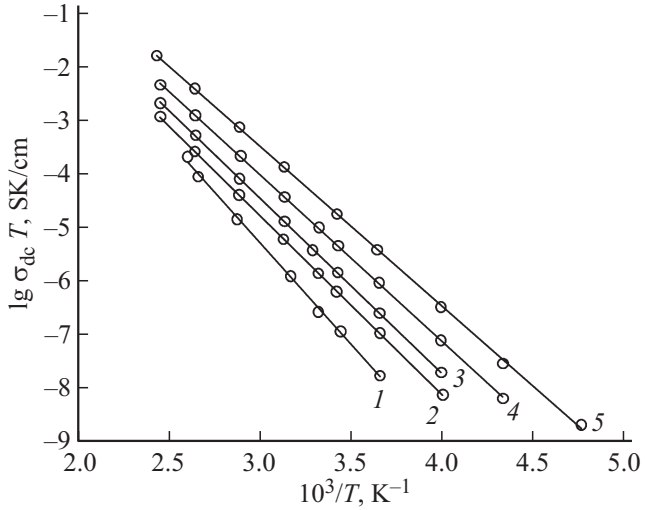

Figure 2. Temperature dependences of ionic conductivity $\lg(\sigma_{dc}T)$, $10^3/T$ for $Ba_{1-x}La_xF_{2+x}$ crystals at x equal to 0.05 (curve *1*), 0.15 (*2*), 0.25 (*3*), 0.325 (*4*), 0.50 (*5*).

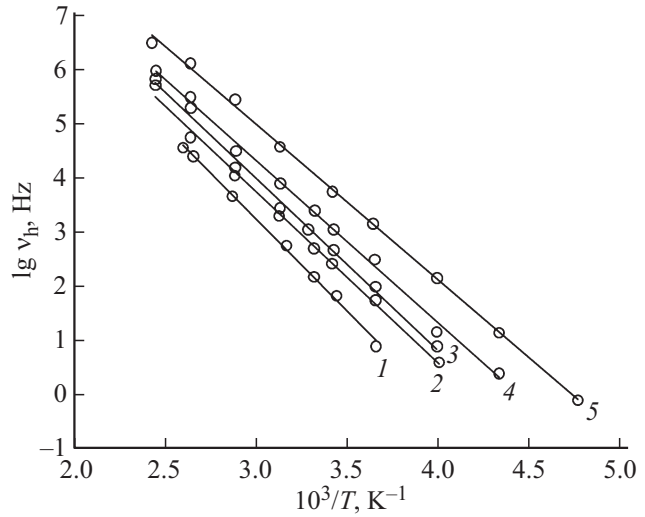

Figure 3. Temperature dependences of charge carrier hopping frequency $\lg\nu_h$, $10^3/T$ for $Ba_{1-x}La_xF_{2+x}$ crystals at x equal to 0.05 (curve *1*), 0.15 (*2*), 0.25 (*3*), 0.325 (*4*), 0.50 (*5*).

that charge carrier concentration does not depend on the temperature ($H_f = 0$) and is defined by the structural mechanism of heterovalent substitutions of Ba^{2+} by La^{3+}. Heterovalent substitutions of Ba^{2+} by La^{3+} result in charge heterogeneity of cation sublattice and spatial heterogeneity of anion sublattice (appearance of additional fluorine ions in interstitial positions). The structurally disordered state of the anionic sublattice is of crystallochemical type and is retained at low temperatures.

When Ba^{2+} are substituted by La^{3+}, interstitial fluorine ions are formed in $Ba_{1-x}La_xF_{2+x}$ fluorite crystals owing to two factors: first, due to compensation of impurity cation overcharge

$$Ba_{Ba}^{\times} \rightarrow La_{Ba}^{\bullet} + F_i', \tag{6}$$

and, second, due to the formation of fluorine vacancies to overcome short cation–fluorine bonds (formation of anti-Frenkel defects):

$$F_F^{\times} \rightarrow V_F^{\bullet} + F_i'. \tag{7}$$

The presence of F_i' ions in interstitial positions 48*i* space group $Fm\bar{3}m$ and vacancies $V_F^{\bullet}$ in main positions 8*c* of fluorite structure $Ba_{0.69}La_{0.31}F_{2.31}$ was detected by neutron- [34,35] and X-ray diffraction [36] methods. This fact indicates that cation-anion clusters $[Ba_8La_6F_{69}]=[Ba_8(R_6F_{37})F_{32}]$ [21,22] with rare-earth clusters $[La_6F_{37}]$ as cores [20] are formed in the solid solution structure. For $Ba_{1-x}La_xF_{2+x}$ crystals, cluster scheme of heterovalent substitutions (block isomorphism) takes place [37]:

$$[Ba_{14}F_{64}]_{Ba_{14}F_{64}}^{\times} \rightarrow [Ba_8La_6F_{69}]_{Ba_{14}F_{64}}^{\bullet} + F_{mob}', \tag{8}$$

where F_{mob}' are interstitial fluorine ions in positions 4*b* space group $Fm\bar{3}m$ outside the cluster. In a microscopic model [1], ionic transport in the concentrated $Ba_{1-x}La_xF_{2+x}$ ($0.05 \le x \le 0.5$) solid solution is associated with delocalized movement of mobile interstitial ions F_{mob}' (charge carriers) located outside structural clusters $[Ba_8La_6F_{69}]$.

Considering (8), concentration of mobile fluorine ions F_{mob}' is equal to

$$n_{mob} = Zx/6a^3, \tag{9}$$

where the number of formula units in the fluorite lattice cell $Z = 4$, x is the mole fraction of LaF_3 in solid solution, a is the lattice cell parameter. Lattice constants $a(x)$ are taken from [14]. For $Ba_{1-x}La_xF_{2+x}$ crystals, charge carrier concentration calculated by equation (9) is given in Table 3 and is 0.4–3.3% of the total number of anions.

Concentrations n_{mob} in the given $Ba_{1-x}La_xF_{2+x}$ crystals are 10^7-10^8 times higher than the concentration of anti-Frenkel defects in the BaF_2 fluorite matrix ($n_{mob} = 9.4 \cdot 10^{12}\,cm^{-3}$ [38] at 400 K), which proves high structural disorder of the anion subsystem of $Ba_{1-x}La_xF_{2+x}$ crystals.

Taking the resulting values of σ_{dc} and n_{mob}, charge carrier mobility μ_{mob} may be assessed:

$$\mu_{mob} = \sigma_{dc}/qn_{mob}. \tag{10}$$

Values of μ_{mob} at 293 and 400 K calculated by equation (10) are listed in Table 3. It can be seen that charge carrier mobility at 400 K $\mu_{mob} = 1.1 \cdot 10^{-7}\,cm^2/(sV)$ in $Ba_{0.5}La_{0.5}F_{2.5}$ superionic crystal is much higher than the interstitial ion mobility F_{mob}' in BaF_2 ($\mu_{int} = 1.1 \cdot 10^{-9}$ crystal [38], $1.0 \cdot 10^{-8}\,cm^2/(sV)$ [39]) and higher than or comparable with the fluorine vacancy mobility $V_F^{\bullet}$ ($\mu_{vac} = 2.2 \cdot 10^{-8}$ [38], $1.4 \cdot 10^{-7}\,cm^2/(sV)$ [40]).

Charge carrier quantity μ_{mob} is given by the Nernst–Einstein relation and defined by charge carrier hopping frequency ν_h and distance d_h

$$\mu_{mob} = q\nu_h d_h^2/6kT. \tag{11}$$

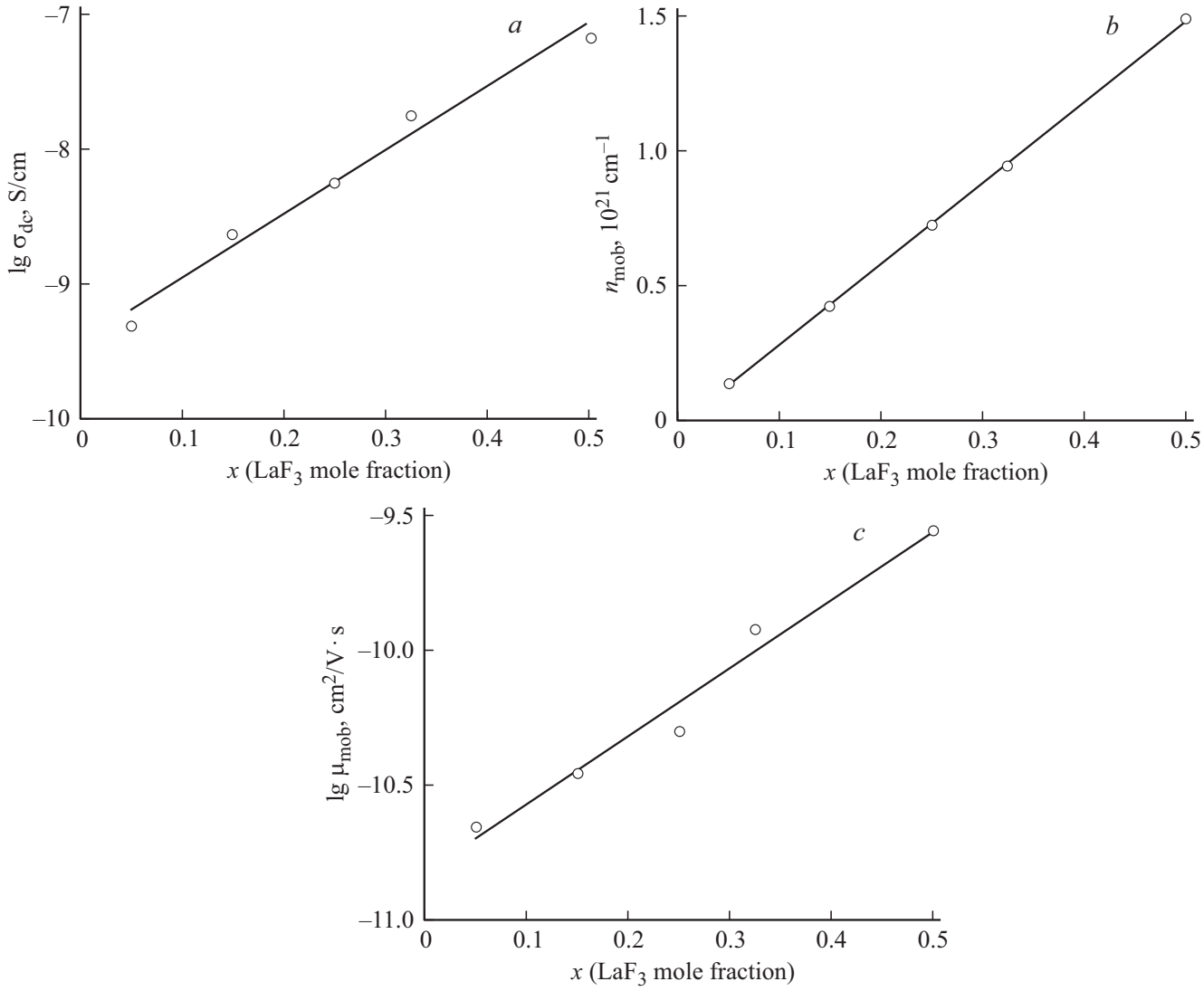

Figure 4. Concentration dependences *a*) of ionic conductivity $\sigma_{dc}(x)$, *b*) concentration $n_{mob}(x)$ and *c*) mobility $\mu_{mob}(x)$ of charge carriers for $Ba_{1-x}La_xF_{2+x}$ crystals $(0.05 \leq x \leq 0.50)$ at 293 K.

Knowing the charge mobility μ_{mob} and frequency ν_h, the hopping distance d_h may be assessed:

$$d_h = \left[6kT\mu_{mob}/q\nu_h\right]^{1/2}. \quad (12)$$

Values of d_h calculated using equations (12) are listed in Table 1 and are equal to 0.8−2 nm.

Figure 4 shows the calculated concentration dependences of ionic conductivity (293 K), concentration and mobility of charge carriers for $Ba_{1-x}La_xF_{2+x}$ crystals at $0.05 \leq x \leq 0.50$. It is shown that dependences $\sigma_{dc}(x)$, $n_{mob}(x)$ and $\mu_{mob}(x)$ are simbasic. When the crystal composition is changed from $x = 0.05$ to 0.5 (by 10 times), σ_{dc}, μ_{mob} and n_{mob} are 136 times, 12.7 times and 10.7 times higher, respectively.

Thus, contributions of mobility $\mu_{mob}(x)$ and concentration $n_{mob}(x)$ of charge carriers to the concentration dependence of „room" conductivity $\sigma_{dc}(x)$ of $Ba_{1-x}La_xF_{2+x}$ superionic conductor crystals are almost the same.

4. Conclusion

Study of the superionic conductivity at the microscopic level is an important challenge for fluoride materials ionics. The study investigates frequency-temperature dependences of alternating current conductivity $\sigma_{ac}(\nu, T)$ of $Ba_{1-x}La_xF_{2+x}$ superionic conductor single-crystals at $0.05 \leq x \leq 0.5$, concentration dependences of microscopic characteristics of ionic transport and discusses the contribution of mobility charge carrier mobility $\mu_{mob}(x)$ and concentration $n_{mob}(x)$ to concentration behavior of ionic conductivity $\sigma_{dc}(x)$.

Heterovalent $Ba_{1-x}La_xF_{2+x}$ solid solution with the fluorite structure is a model system for nonstoichiometric fluoride superionic materials. In $Ba_{1-x}La_xF_{2+x}$ superionic conductor, interstitial ions F'_{mob} are charge carriers. These ions are formed by heterovalent substitutions of $[Ba_{14}F_{64}]$ matric fragments by $[Ba_8La_6F_{69}]$ structural clusters. Fre-

quency dependences of dynamic conductivity $\sigma_{ac}(\nu)$ were used to calculate charge carrier hopping frequencies $\nu_h(x)$ and direct current conductivity $\sigma_{dc}(\nu)$ in $Ba_{1-x}La_xF_{2+x}$ single-crystals with composition variation from $x = 0.05$ to 0.5. Crystal-physical model was used to calculate concentration dependences of charge carrier mobility $\mu_{mob}(x)$, concentration $n_{mob}(x)$ and hopping length $d_h(x)$. It has been found that the contribution to „room" conductivity $\sigma_{dc}(x)$ of $Ba_{1-x}La_xF_{2+x}$ crystals ($0.05 \leq x \leq 0.50$) is approximately equally attributed to an increase in charge carrier concentration and mobility.

Acknowledgments

The author is grateful to E.A. Krivandina and Z.I. Zhmurova for the provided crystals for the study.

Funding

The study was carried out under the State Work-Order of Federal Scientific Research Center „Crystallography and Photonics", Russian Academy of Sciences.

Conflict of interest

The author declares that he has no conflict of interest.

References

[1] N.I. Sorokin, D.N. Karimov. Phys. Solid State **63**, *12*, 1821 (2021).
[2] N.I. Sorokin. Phys. Solid State **60**, *4*, 714 (2018).
[3] N.I. Sorokin. Phys. Solid State **57**, *7*, 1352 (2015).
[4] N.I. Sorokin, B.P. Sobolev. Phys. Solid State **50**, *3*, 416 (2008).
[5] X. Cheng, S. Wang, X. Lin. IOP Conf. Ser.: Mater. Sci. Eng. **678**, *1*, 012148 (2019).
[6] F. Preishuber-Pflügl, P. Bottke, V. Pregarther, B. Bitschnau, M. Wilkening. Phys. Chem. Chem. Phys. **16**, *20*, 9580 (2014).
[7] A. Düvel, J. Bednarcik, V. Šepelák, P. Heitjans. J. Phys. Chem. C **118**, *13*, 7117 (2014).
[8] C. Rongeat, M.A. Reddy, R. Witter, M. Fichtner. J. Phys. Chem. C **117**, *10*, 4943 (2013).
[9] N.I. Sorokin, M.W. Breiter. Solid State Ionics **99**, *3–4*, 241 (1997).
[10] A.K. Ivanov-Shits, N.I. Sorokin, P.P. Fedorov, B.P. Sobolev. Solid State Ionics **31**, *4*, 269 (1989).
[11] K.E. Rammutla, J.R. Comins, R.M. Erasmus, T.T. Netshisaulu, P.E. Ngoepe, A.V. Chadwick. Radiation Effects and Defects in Solids **157**, *6–12*, 783 (2002).
[12] H.W. den Hartog, J.C. Langevoort. Phys. Rev. B **24**, *6*, 3547 (1981).
[13] K.E.D. Wapenaar, J.L. van Koesveld, J. Schoonman. Solid State Ionics **2**, *3*, 145 (1981).
[14] B.P. Sobolev, N.L. Tkachenko. Less-Common Metals **85**, 155 (1982).
[15] B.P. Sobolev, Z.I. Zhmurova, V.V. Karelin, E.A. Krivandina, P.P. Fedorov, T.M. Turkina. Rost kristallov **16**, 58 (1988). (in Russian).
[16] A.Yu. Kuznetsov, A.B. Sobolev, A.N. Varaksin, J. Andriessen, C.W.E. van Eijk. Phys. Solid State **45**, *5*, 838 (2003).
[17] I.V. Murin, A.V. Glumov, V.M. Reiterov. Fizika tverdogo tela. **23**, *3*, 702 (1981). (in Russian).
[18] K.E.D. Wapenaar, C.R.A. Catlow. Solid State Ionics **2**, *4*, 245 (1981).
[19] F.A. Kröger. The Chemistry of Inperfect Crystals. North-Holland Publishing Company, Amsterdam (1964). 1039 p.
[20] D.J.M. Bevan, O. Greis, J. Strähle. Acta Cryst. A **36**, *Part 6*, 889 (1980).
[21] E.A. Sulyanova, B.P. Sobolev. Cryst. Eng. Commun. **24**, *20*, 3762 (2022).
[22] A.M. Golubev, V.I. Simonov. Kristallografiya **31**, *478*, 1986 (1990). (in Russian).
[23] S.A. Kazanskii, A.I. Ryskin. Phys. Solid State **44**, *8*, 1415 (2002)
[24] L.K. Aminov, I.N. Kurkin, S.P. Kurzin, I.A. Gromov, G.V. Mamin, R.M. Rakhmatullin. Phys. Solid State **49**, *11*, 2086 (2007).
[25] F. Kadlec, F. Moussa, P. Simon, G. Gruener, B.P. Sobolev. Mater. Sci. Eng. B **57**, *3*, 234 (1999).
[26] B.A. Maksimov, Kh. Solans, A.P. Dudka, E.A. Genkina, M. Badria-Font, I.I. Buchinskaya, A.M. Golbev, A.A. Loshmanov, V.I. Simonov, M. Font-Altaba, B.P. Sobolev. Kristallografiya **41**, *1*, 51 (1996). (in Russian).
[27] S.N.S. Reddy, R.A. Rapp. J. Electrochem. Soc. **126**, *11*, 2023 (1979).
[28] D. Jakes, J. Kaplan, V. Trnovcova, B.P. Sobolev. 3th Asian Conf. on Solid State Ionics. Varanasi (1992). P. 147.
[29] T. Takami, C. Pattanathummasid, A. Kutana, R. Asahi. J. Phys.: Condens. Matter **35**, *29*, 293002 (2023).
[30] A.W. Xiao, G. Galatolo, M. Pasta. Joule **5**, *11*, 2823 (2021). https://doi.org/10.1016/j.joule.2021.09.016
[31] D.P. Almond, C.C. Hunter, A.R. West. J. Mater. Sci. **19**, *10*, 3236 (1984).
[32] N.I. Sorokin, B.P. Sobolev. Phys. Solid State **60**, *12*, 2450 (2018).
[33] I.Yu. Gotlib, I.V. Murin, I.V. Piotrovskaya, E.N. Brodskaya. Neorgan. materialy **38**, *3*, 358 (2002). (in Russian).
[34] L.P. Otroshchenko, V.B. Aleksandrov, L.A. Muradian, V.A. Sarin, B.P. Sobolev. Butll. Soc. Cat. Cien. **12**, *2*, 383 (1991).
[35] N.H. Andersen, K.N. Clausen, J.K. Kjems, J. Schoonman. J. Phys. C **19**, *14*, 2377 (1986).
[36] E.A. Sulyanova, D.N. Karimov, B.P. Sobolev. Crystals **11**, *4*, 447 (2021).
[37] N.I. Sorokin, A.M. Golubev, B.P. Sobolev. Crystallogr. Rep. **59**, *2*, 238 (2014).
[38] W. Bollmann. Cryst. Res. Technol. **16**, *9*, 1039 (1981).
[39] P.W.M. Jacobs, S.H. Ong. Cryst. Lattice Defects **8**, 177 (1980).
[40] E. Barsis, A. Taylor. J. Chem. Phys. **48**, *10*, 4357 (1968).

Translated by E.Ilinskaya